A CRISPR-associated factor Csa3a regulates DNA damage repair in Crenarchaeon *Sulfolobus islandicus*

Zhenzhen Liu[1], Mengmeng Sun[2], Jilin Liu[1], Tao Liu[1], Qing Ye[1], Yingjun Li[1] and Nan Peng [ID][1,*]

[1]State Key Laboratory of Agricultural Microbiology, College of Life Science and Technology, Huazhong Agricultural University, Wuhan, 430070, P.R. China and [2]Department of Biology, University of Copenhagen, DK-2200 Copenhagen N, Denmark

ABSTRACT

CRISPR−Cas system provides acquired immunity against invasive genetic elements in prokaryotes. In both bacteria and archaea, transcriptional factors play important roles in regulation of CRISPR adaptation and interference. In the model Crenarchaeon *Sulfolobus islandicus*, a CRISPR-associated factor Csa3a triggers CRISPR adaptation and activates CRISPR RNA transcription for the immunity. However, regulation of DNA repair systems for repairing the genomic DNA damages caused by the CRISPR self-immunity is less understood. Here, according to the transcriptome and reporter gene data, we found that deletion of the *csa3a* gene downregulated the DNA damage response (DDR) genes, including the *ups* and *ced* genes. Furthermore, *in vitro* analyses demonstrated that Csa3a specifically bound the DDR gene promoters. Microscopic analysis showed that deletion of *csa3a* significantly inhibited DNA damage-induced cell aggregation. Moreover, the flow cytometry study and survival rate analysis revealed that the *csa3a* deletion strain was more sensitive to the DNA-damaging reagent. Importantly, CRISPR self-targeting and DNA transfer experiments revealed that Csa3a was involved in regulating Ups- and Ced-mediated repair of CRISPR-damaged host genomic DNA. These results explain the interplay between Csa3a functions in activating CRISPR adaptation and DNA repair systems, and expands our understanding of the lost link between CRISPR self-immunity and genome stability.

INTRODUCTION

CRISPR−Cas (clustered regularly interspaced short palindromic repeats and CRISPR-associated) systems are prokaryotic immune systems that protect Bacteria and Archaea against invasive viruses and plasmids (1,2). These adaptive immune systems are grouped into two major classes and six types (I−VI) (3). Class 1 CRISPR−Cas systems (Types I, III and IV) utilize the interference machinery composed of multiple Cas proteins, whereas class 2 systems (Types II, V and VI) employ a single Cas protein for interference. CRISPR immunity occurs in three functional stages, including adaptation (uptake of new spacers), crRNA biogenesis (transcription and processing of CRISPR RNA), and interference (nucleic acid-targeting and cleavage) (4,5). The conserved Cas1 and Cas2 proteins are essential in the adaptation stage to integrate spacers from invaders into CRISPR arrays (6). For instance, in the *Sulfolobus islandicus* subtype I-A system, the *cas1* and *cas2* genes, as well as the additional adaptation *cas* genes (*csa1* and *cas4*) are transcriptionally activated for CRISPR adaptation via the CRISPR-associated factor Csa3a (7,8). However, CRISPR adaptation, in most cases, select spacers from host genomic DNA, in addition to the mobile genetic elements (MGEs) (8–10), thereby inducing self-immunity.

At the interference stage, CRISPR−Cas systems introduce DNA breaks at the target sites, both on the invasive and host genomic DNA (11). Damages on the genomic DNA caused by CRISPR interference, other environmental or endogenous factors could be repaired to maintain genome stability. There have been many studies on DNA damage repair in bacteria, archaea and eukaryotes, among which a unique regulatory network called DNA damage response (DDR) has been revealed (12,13). The regulatory mechanism of DDR governed by the RecA and LexA proteins is the best representative by the SOS response and is conserved in numerous bacteria (14). To ensure an effective and timely DNA damage repair in cells, the DDR mechanism shows some common characteristics, including rapid identification of DNA damage signals, after which a series of cellular events occur coordinatively, for example, inhibition of DNA replication, cell cycle arrest and activating expression of DNA repair enzymes (15). The Crenar-

*To whom correspondence should be addressed. Tel: +86 27 8728 1267; Fax: +86 27 8728 0670; Email: nanpengbio@live.cn; nanp@mail.hzau.edu.cn

chaon *Sulfolobus* species encode specific DNA repair systems which transfer chromosome DNA between *Sulfolobus* cells for homologous recombination (16). Particularly, these systems rely on cell aggregation induced by the Ups (UV-inducible pili of *Sulfolobus*) post DNA damage (17,18), and the Ced (Crenarchaeal system for exchange of DNA) system directly function in the transfer of chromosomal DNA among cells (16). DNA transferred via the Ced system into cells is used as the donor for homologous recombination repair of the damaged DNA (16).

Ups- and Ced-mediated DNA repair in *Sulfolobus* species is efficiently regulated. Recent reports have revealed that Cdc6–2 is a central factor for activation of several DDR genes including *ups* and *ced* genes, DNA polymerase II (*dpo2*), homologous recombination repair genes, and the *tfb3* gene which encodes the secondary DDR regulator (19,20). Besides, Cdc6–2 represses expression of genes associated with cell division, DNA replication initiation, and genome segregation (21).

In *S. islandicus*, the CRISPR-associated factor Csa3a has been revealed to activate the expression of adaptation *cas* gene, CRISPR RNA and DNA repair genes, including helicase *herA*, nuclease *nurA* and *dpo2* genes (8). However, it remains an open question on whether Csa3a regulates DDR pathways for DNA damage repair in *Sulfolobus*. Herein, we assessed whether Csa3a activates expression of *ups* and *ced* operons, as well as *cdc6–2* and *tfb3* genes, and unveiled the crosstalk between the CRISPR−Cas system and DNA repair pathways in the Crenarchaeon *S. islandicus*.

MATERIALS AND METHODS

Cell growth and DNA damage treatment

Sulfolobus islandicus strains, including the wild-type (E233S) and the derived strains, are listed in Supplementary Table S1. These strains were cultured at 78°C in the SCV medium (basal medium supplemented with 0.2% sucrose, 0.2% casamino acids and 1% vitamin solution), or SCVU medium (SCV medium with addition of 20 μg/ml uracil at a final concentration) (22).

Sulfolobus genomic DNA damage treatment using 4-nitroquinoline-1-oxide (NQO), which mimics UV radiation, was performed as previously described (23). Briefly, NQO dissolved in DMSO solution was added to *Sulfolobus* cultures at the early exponential growth phase (OD$_{600}$ = 0.2) to a final concentration specified in each experiment. Cell concentration was determined at OD$_{600}$ during incubation, and cell samples were taken for aggregation assay, cell viability assay, RNA extraction, and flow cytometry analysis.

Protein expression and purification

Expression and purification of the Csa3a protein were conducted as described previously (7).

Transcriptome analysis

Strains (two biological repeats for each strain) for transcriptome analysis were cultured to log phase (OD$_{600}$ = 0.2). Thereafter, a 1 ml culture of each strain was transferred to 100 ml fresh SCVU medium in 250-ml flasks. Exponentially growing cultures of *S. islandicus* E233S (the wild-type strain, WT,) and Δ*csa3a* were diluted to OD$_{600}$ = 0.2 and cultured in the presence or absence of 2 μM NQO for 6 h. Then, total RNA was extracted using the Trizol reagent (Invitrogen, Carlsbad, CA, USA). Genomic DNA in the total RNA sample was removed using DNase I (Roche, Basel, Switzerland). The quality and quantity of purified total RNA were determined by measuring the absorbance at 260 and 280 nm using a NanoDrop ND-1000 spectrophotometer (Labtech, Wilmington, MA, USA). Total RNA integrity was verified by electrophoresis on a 1.5% agarose gel. A total of 3 μg RNA per sample was used as input material for cDNA library preparations. Sequencing libraries were generated using the NEBNext Ultra™ RNA Library Prep Kit for Illumina (NEB, USA) following the manufacturer's recommendations, and index codes were added to assign sequences to each sample. First-strand cDNA synthesis was performed using random hexamer primers and M-MuLV Reverse Transcriptase (RNase H−). Subsequently, second-strand cDNA synthesis was performed using DNA polymerase I and RNase H, followed by 15 cycles of PCR enrichment. Sequencing was performed with an Illumina HiSeq2000 instrument. Raw data were initially processed to obtain clean reads by eliminating adapter sequences and low-quality bases. Clean reads were aligned to the reference genome sequence of *S. islandicus* REY15A (GenBank Accession No. NC_017276). An index of the reference genome was built using Bowtie software v2.0.6, and paired-end clean reads were aligned to the reference genome using TopHat software v2.0.9. To count the number of reads mapped to each gene, HTSeq software v0.6.1 was used, following which the reads per kilobase per million mapped reads (RPKM) for each gene was calculated based on the length of the gene and the number of reads mapped to the gene. Each strain was sequenced in duplicate. To determine the expression level of each gene in different groups, transcript expression levels were expressed as the RPKM. Next, *P*-values were used to identify differentially expressed genes (DEGs) between the 2 groups using the chi-squared test (2 × 2), and the significance threshold of the *P*-value in multiple tests was set based on the false discovery rate (FDR). Furthermore, Fold-changes (log$_2$[RPKM1/RPKM2]) were estimated according to normalized gene-expression levels. Threshold for DEGs was set at *P*-values < 0.01 and log$_2$ fold-change >1 (FDR < 0.05). Transcriptome data were deposited in the SRA database under Accession PRJNA608153. The DEGs are listed in Supplementary Table S2.

Electrophoretic mobility shift assay

PCR was used to generate probes for electrophoretic mobility shift assay (EMSA) using one of the primers with 5′-end HEX-label (Supplementary Table S3). PCR products of the probes were first cloned into the T-vector as the template for inverse PCR to introduce mutations at the desired sites. Mutated probes were amplified from above plasmids introduced with mutations using one of the primers with 5′-end HEX-label. Then, the PCR products were purified in 6% native polyacrylamide gel electrophoresis (PAGE) for EMSA.

EMSA binding reactions (15 μl) containing 5 ng/μl of HEX-labeled probes and different concentrations of Csa3a protein (as described in the figure legends) were incubated for 20 min at 40°C in the binding buffer [20 mM Tris–HCl, pH8.0, 50 mM KCl, 5% glycerol, 1 mM ethylenediaminetetraacetic acid, 1 mM dithiothreitol, 5 ng/μl poly(dI-dC)]. For the specific competition, increasing amounts of unlabeled specific probes were added to the reaction mixture. Thereafter, samples were loaded onto a 4% low melting agarose gel buffered with 1× TAE solution. DNA–protein complexes were separated at 200 V for 40 min and the resulting bands was detected using a FUJIFILM scanner (FLA-5100).

Localized surface plasmon resonance analysis

PCR was used to generate the probes for the localized surface plasmon resonance (LSPR) analysis using the primers listed in Supplementary Table S3. PCR products were purified through ethanol precipitation. The Csa3a protein was immobilized on the chip with different titers of probes in the mobile phase, as indicated in the figure legends. The kinetic parameters of the binding reactions were calculated and analyzed by Trace Drawer software (Ridgeview Instruments AB, Sweden) and One to One fitting model.

Flow cytometry analysis

The flow cytometry analysis was conducted as described previously (23). Briefly, 300 μl of *Sulfolobus* cells were fixed with 700 μl of absolute ethanol and stored at 4°C for 12 h. Then, fixed cells were collected through centrifugation at 2, 800 rpm for 20 min and washed with 1 ml of 10 mM Tris–NaCl buffer, pH 7.5, with 10 mM $MgCl_2$. Cells were collected again and stained with 40 μg/ml ethidium bromide (Sigma-Aldrich, St. Louis, MO, USA) and 100 μg/ml mithramycin A (Apollo chemical, Tamworth, UK). We analyzed the stained cell samples in an Apogee A40 cytometer (Apogeeflow, Hertfordshire, UK) equipped with a 405 nm laser. A dataset of at least 60 000 cells were collected for each sample.

Cell aggregation assay

Cell aggregation in *S. islandicus* cultures was estimated through direct microscopy of cell aggregates in fresh cultures, as previously described (19). Briefly, each strain was cultured in the absence or presence of 2 μM NQO for 12 h, after which aliquots were placed on glass slides, covered with coverslips and directly observed under a Nikon Eclipse 80i microscope (Nikon, Kobe, Japan). Data were collected from at least 24 fields of view images and more than 1000 single cells for each sample. For each analysis, three independent growth experiments were conducted.

Report gene assay

Reporter plasmids were constructed using the *Sulfolobus–E. coli* shuttle vector pSeSD with the *S. solfataricus* galactosidase gene (*lacS*) as the reporter gene (24). For this experiment, we selected the promoters of the single DDR genes or the first genes of the DDR operons (SiRe_1878: *upsX*, SiRe_1879: *upsE*, SiRe_1881: *upsA*, SiRe_1316: *cedA1*, SiRe_1857: *cedB*, SiRe_1717: *tfb3* and SiRe_1231: *cdc6–2*) that were up-regulated in the *csa3a* overexpression cells. Promoter fragments of these genes were amplified from *S. islandicus* REY15A genomic DNA using Phanta DNA Polymerase (Vazyme, Nanjing, China), and the primers listed in Supplementary Table S3. The PCR products (ca. 200 bp) were purified using the Cycle-Pure kit (Omega Bio-Tek, USA). Purified DNAs were digested and inserted into the pSe-*lacS* vector (25) to yield the reporter plasmids: pSe-*upsX-lacS*, pSe-*upsE-lacS*, pSe-*upsA-lacS*, pSe-*cedA1-lacS*, pSe-*cedB-lacS*, pSe-*tfb3-lacS* and pSe-*cdc6–2-lacS* (Supplementary Table S1).

These reporter gene plasmids were electroporated into *S. islandicus* wild-type (E233S) and Δ*csa3a* strains, respectively. Three single colonies of each transformant were selected and cultured for 6 h in SCV either in the presence or absence of 2 μM NQO. Cell mass was collected for each strain and used to prepare the cellular extracts. The protein content of the cellular extracts was determined by microBCA Protein Assay Reagent (Thermo Scientific), whereas the β-galactosidase activity was determined as previously described (24).

Cell viability analysis

We estimated the cell viability of *Sulfolobus* cultures by determining their colony formation units (CFU)/ml culture. Exponentially growing cultures of *S. islandicus* (OD_{600} = 0.2) were treated with NQO to a final concentration of 2 μM and incubated for 6 h. Then, using 1 ml of culture, cells were pelleted by centrifugation and re-suspended in 1 ml fresh SCVU medium. The resulting cell suspensions were serially diluted and plated using the two-layer plating method. Exactly 100 μl of the diluted samples were plated onto gelrite plates in triplicate. Colonies appearing on plates after 7 days of incubation were counted, to determine CFUs/ml culture.

Plate titration experiment

The plate titration experiment of *Sulfolobus* was estimated by determining the density of the lawns on the plate. Exponentially growing cultures of *S. islandicus* (OD_{600} = 0.2) were treated with NQO with a final concentration of 2 μM and incubated for 48 h. Then, using 1 ml of culture, cells were serially diluted, and 10 μl of the diluted sample was dripped on the SCVU plate and incubated at 78°C for 2 days.

DNA transfer and repair assays

DNA transfer assay was conducted as described previously (16), with modification. Targeting plasmid pT*cas5* was constructed by cloning an oligonucleotide matching the protospacer on the *cas5* gene in a mini-CRISPR cassette (Repeat-Spacer-Repeat) on the pSeSD plasmid. Then, 1 μg of pT*cas5* plasmid was electroporated into 50 μl competent cells of *S. islandicus* wt (Δ*pyrEF*Δ*lacS*)

or Δ*csa3a* (Δ*pyrEF*Δ*lacS*Δ*csa3a*) cells. After electroporation, 1 ml preheated medium was added into the culture containing the transformed cells. The mixed cultures were incubated with or without 2 ml of preheated Δ*cas5* (Δ*pyrEF*Δ*lacS*Δ*cas5*) mating partner cells (OD_{600} = 0.5) for 2 h at 78°C, then, plated on the SCV medium without uracil at 78°C for 6 days. We calculated increased folds of transformation efficiencies of wt or Δ*csa3a* cells incubated with Δ*cas5* partner cells compared with that of wt or Δ*csa3a* cells ($E_{[wt::pTcas5+\Delta cas5]}/E_{wt::pTcas5}$ or $E_{[\Delta csa3a::pTcas5+\Delta cas5]}/E_{\Delta csa3a::pTcas5}$; E: transformation efficiency), respectively. Deletion of the *cas5* gene locus on the chromosomes of the single colonies of wt::pT*cas5* × Δ*cas5* or Δ*csa3a*::pT*cas5* × Δ*cas5* conjugants were determined by PCR analysis.

RESULTS

Csa3a acted as a transcriptional activator for the DDR genes

The *S. islandicus* strain REY15A carries a subtype I-A adaptation module consisting of the *csa1* (SiRe_0760), *cas1* (SiRe_0761), *cas2* (SiRe_0762) and *cas4* (SiRe_0763) genes, which are regulated by a factor encoded by the CRISPR-associated *csa3a* gene (Figure 1A) (7). Besides, this strain carries an *ups* operon and a *ced* cluster (Figure 1B and C), encoding pili which aid in cell aggregation (18) and encoding a membrane system for DNA transfer, thereby mediating DNA damage repair via homologous recombination (16).

Upon re-analysis of our previous transcriptome data (8), we found that most of the DDR genes, including the *ups* and *ced* genes, as well as the *cdc6-2* and *tfb3* genes, were significantly up-regulated in the *csa3a* overexpression strain (Supplementary Table S4). In this study, we revealed that most of these genes were correspondingly down-regulated in the *csa3a* deletion strain based on the transcriptome data (Table 1). These results inferred that the Csa3a factor acts as a transcriptional activator for the DDR genes in *S. islandicus*.

A previous report indicated that DDR genes were induced by NQO reagent (23), we observed a similar phenomenon based on our transcriptome data (Table 1). NQO induced-expression of DDR genes is much stronger than Csa3a induced (Table 1). NQO also induced DDR expression in the *csa3a* gene deletion strain (Table 1), indicating Csa3a might not be essential for DDR induction upon NQO treatment. However, transcriptome data for the *csa3a* deletion strain and the wild-type strain both treated with NQO revealed that transcription of *upsA* and *tfb3* genes (Table 1) were significantly down-regulated in *csa3a* deletion strain (Table 1). The later was essential for the regulation of DDR genes (19). Conclusively, these findings indicated Csa3a might play an important, but not essential, role in the regulation of DDR genes in *S. islandicus*.

Csa3a specifically bound to the DDR gene promoters

To assess whether Csa3a directly bound to the promoters of the DDR genes to regulate their expression, DNA fragments of the *upsX* (SiRe_1878), *upsE* (SiRe_1879), *upsA*

(SiRe_1881), *cedA1* (SiRe_1316), *cedB* (SiRe_1857), *cdc6-2* (SiRe_1231) and *tfb3* (SiRe_1717) promoters were used as probes for EMSA and LSPR experiments. In our previous investigation, we found that Csa3a specifically bound to *csa1* promoter and the leader sequence, and deletion of or mutations at the binding sites completely abolished the binding (7,8). Here, the truncated leader sequence (−94 to −15, relative to the first repeat) with deletion of the confirmed Csa3a binding site (8) was used as the non-specific probes, and no shift was found in EMSA experiments using Csa3a protein and the non-specific probe (Supplementary Figure S1). Then, we assessed the Csa3a-binding ability using the full-length promoters of the *upsA* (198 bp), *upsX* (227 bp), *upsE* (300 bp), *cedA1* (214 bp), *cedB* (198 bp), *cdc6-2* (200 bp) and *tfb3* (200 bp), upstream of the start codon since the transcriptional start sites were not determined yet. An increase in signal intensity of the retarded bands was parallel with increasing Csa3a amounts (40, 80 or 120 ng/μl) in each EMSA experiment (Figure 2A). On the other hand, the signal of retarded band for each EMSA experiment was completely abolished for all tested promoters in the presence of 2- or 4-fold excess of unlabeled specific competitor DNA (cold probe) (Figure 2A). Notably, a DNA motif similar to the UV-responsive motif (26) was identified for all tested promoters. The mutated promoters with transversion mutation at the UV-responsive motif and its flanking region formed a weak shift band with the Csa3a regulator (40, 80 or 120 ng/μl) in EMSA experiment (Figure 2A). Further, the LSPR results showed different K_D values for the interaction between Csa3a and each wild-type promoter or the mutant promoters (with mutations at the UV-responsive motif and the flanking sequence) (Figure 2B). All LSPR analysis revealed that Csa3a strongly bound to the full-length promoters with K_D values ranging from 0.29 to 1.30 μM (Figure 2B). Generally, the K_D values for the binding between the mutant promoters and Csa3a showed a lower affinity (1–2 orders of magnitude) compared to that between the wild-type promoters and Csa3a (Figure 2B). All LSPR raw data were summarized in Supplementary Table S5. It should be noticed that we previously demonstrated that Csa3a strongly bound a palindromic DNA sequence on the *csa1* promoter and the leader sequence (7,8). However, this DNA motif was not identified on the DDR gene promoters. This might explain the relative weak interaction between the Csa3a factor and the DDR gene promoters, and explain that mutations have a slight effect on their binding in the EMSA and LSPR analyses. Taken together, the EMSA and LSPR results and the transcriptome data indicated that Csa3a specifically binds to these DDR gene promoters to activate their transcription.

Deletion of the *csa3a* gene significantly reduced the promoter activities of the DDR genes

To assess whether Csa3a could regulate the DDR gene expression *in vivo*, promoter fragments of these genes (*upsX*, *upsE*, *upsA*, *cedA1*, *tfb3* and *cdc6-2*) were used in the reporter gene assay (Figure 3A). These promoters were cloned at the immediate upstream of the *lacS* gene, encoding a β-galactosidase, to control its transcription in an
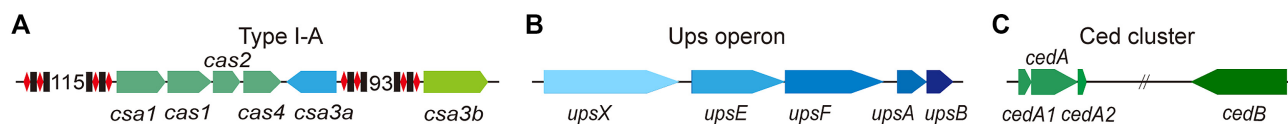
Figure 1. Organization of CRISPR adaptation module (**A**), *ups* (**B**) and *ced* (**C**) operons in *S. islandicus* REY15A. The adaptation module encodes four genes essential for CRISPR adaptation of subtype I-A system. Diamonds and rectangles in the CRISPR arrays represent repeats and spacers; respectively, 115 and 93 are the total numbers of spacers in each CRISPR array. The *ups* cluster: *upsX*, encodes a protein with unknown function; *upsE*, encodes a secretion ATPase; *upsF*, encodes an integral membrane protein; and *upsA* and *upsB*, encode two pili subunits. The ced cluster: *cedA1* and *cedA2*: encode two small transmembrane proteins; *cedA*: encodes a larger transmembrane protein; *cedB*: encodes a HerA/VirB4 homolog.

Table 1. Transcriptional changes (log$_2$-fold) of DNA damage response genes in *S. islandicus* according the transcriptome data

Gene ID	Annotation	Δ*csa3a* vs wt	Δ*csa3a*+NQO vs Δ*csa3a*	Wt+NQO vs wt	Δ*csa3a*+NQO vs wt+NQO
DNA transfer					
SiRe_1878	*upsX*	-	6.29	5.54	-
SiRe_1879	*upsE*	−2.07	7.81	6.35	-
SiRe_1880	*upsF*	−1.30	6.71	5.65	-
SiRe_1881	*upsA*	−2.21	7.54	6.54	−1.16
SiRe_1882	*upsB*	−1.79	7.39	6.49	-
SiRe_1316	*cedA1*	-	6.59	6.38	-
SiRe_1317	*cedA2*	−0.96	6.64	6.06	-
SiRe_1857	*cedB*	−0.93	5.75	5.47	-
Transcriptional regulation					
SiRe_1231	*cdc6-2*	-	3.46	3.53	-
SiRe_1717	*tfb3*	−1.84	6.55	5.89	−1.12
SiRe_0764	*csa3a*	NA	NA	−2.51	NA

'-': Unchanged; NA: not apply.
Significance: log$_2$-fold change >1.

E. coli–Sulfolobus shuttle vector (Figure 3A) (24). Specific β-galactosidase activities demonstrated that the *csa3a* gene deletion significantly reduced the promoter activities of all tested DDR genes without NQO treatment (Figure 3B). However, *csa3a* gene deletion did not significantly impact the expression of these genes after NQO treatment, except for the *cdc6-2* gene (Figure 3B). All raw data for reporter gene assay are summarized in Supplementary Table S6. These findings inferred Csa3a is a key factor in the regulation of the DDR gene expression probably without or with less environmental stresses (e.g. UV radiation or NQO treatment). Moreover, it was suggested that Csa3a could directly regulate the DDR genes or indirectly regulate them via regulation of the *cdc6-2* gene, which was the central factor that regulated DDR gene expression (21).

Deletion of the *csa3a* gene reduced DNA damage-induced cell aggregation

To assess the impact of the Csa3a regulator on Ups–mediated cell aggregation, *S. islandicus* wild-type (WT) and the *csa3a* deletion cells were cultured in presence or absence of 2 μM NQO for 12 h, after which cell samples were examined microscopically. Cell aggregation was observed for neither wild-type strain nor Δ*csa3a* strain at all tested time points without NQO treatment (Figure 4A). On the contrary, the aggregation of wild-type cells treated with NQO increased with growth times (Figure 4A). At the early time point post-NQO treatment (6 h), the aggregates contained 3–6 cells. However, at 12 h, the number of aggregates reached 30 cells in the wild-type sample (Figure 4A). The *csa3a* deletion cells showed a few aggregates at 12 hours

post-NQO treatment, the aggregates contained 3–5 cells at 6 h, and were less than 10 cells at 12 h in the *csa3a* deletion strains (Figure 4A).

Following the microscopic figures, quantitative data (raw data shown in Supplementary Table S7) showed that both strains formed no aggregates at different time points without NQO treatment, however, 20.73% and 50.9% of wild-type cells aggregated. Contrarily, 12.12% and 26.86% of cells of *csa3a* deletion strain aggregated at 6- and 12-h post-NQO treatment (Figure 4B). These findings concurred with results of transcriptome and reporter gene data which indicated that lack of the *csa3a* gene reduced expression of *ups* genes and eventually caused less cell aggregation after NQO treatment.

Deletion of the *csa3a* gene reduced cell viability upon NQO treatment

A recent study revealed that Cdc6-2 affect cell viability in the Ups- and Ced-mediated DDR pathway (21). In this study, we cultured *S. islandicus* wild-type, Δ*csa3a,* and Δ*cdc6–2* strains for 48 h in the medium with or without 2 μM NQO. Then, cells were analyzed by flow cytometry. DNA-less cells were observed for almost all the strains in the NQO treated cultures, and the population of DNA-less cells was proportional to the time of NQO exposure (Figure 5A). Significantly, the Δ*cdc6-2* strain produced many cells with one chromosome (G1 cells), while the population of DNA-less cells with the Δ*csa3a* strain was more than that in the wild-type and Δ*cdc6–2* cells from 6 to 12 h post NQO treatment (Figure 5A). Moreover, in the *csa3a* deletion and wild-type cells, there were a few G1 cells and more G2 cells
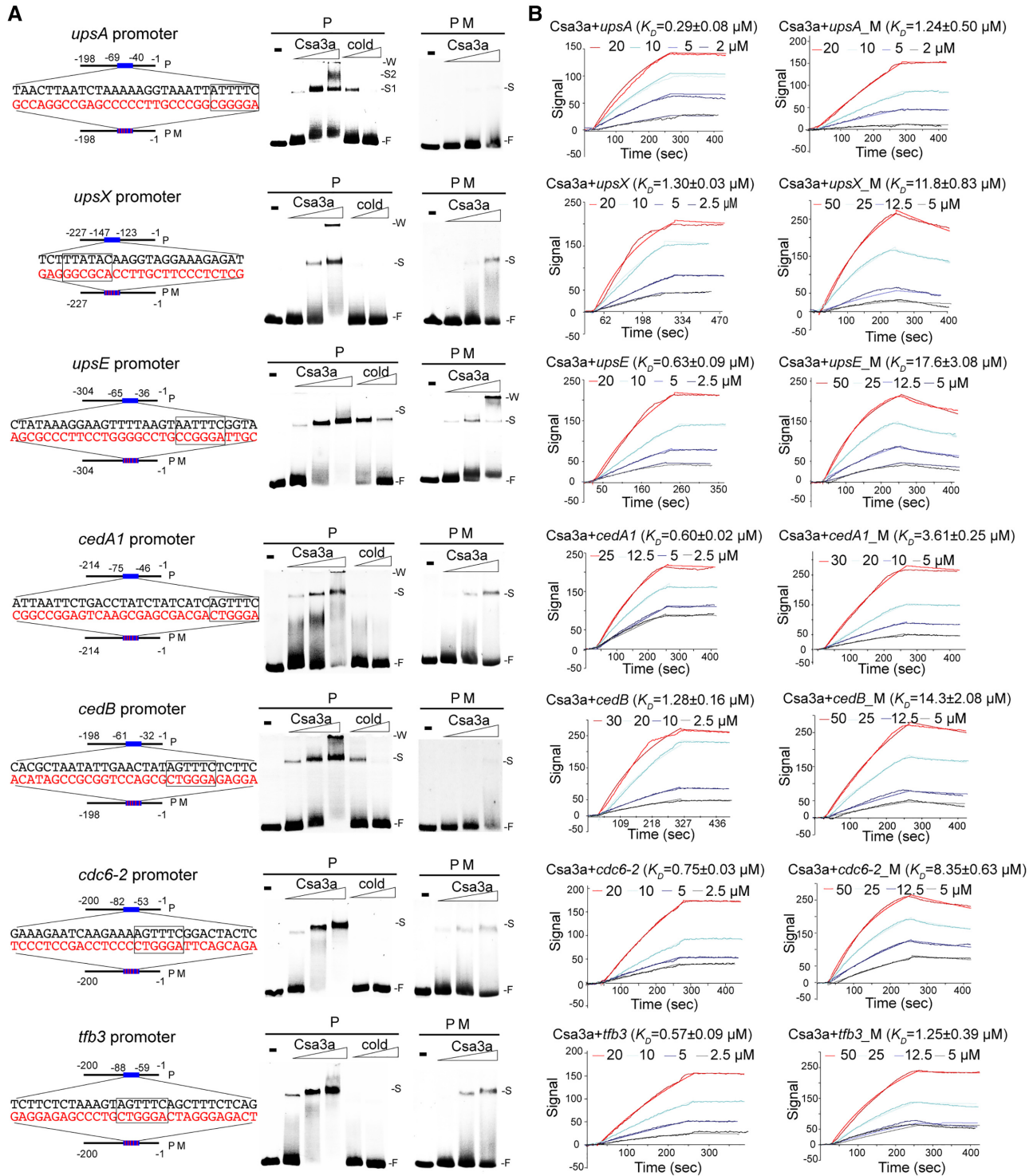
Figure 2. Analysis of Csa3a binding with the promoters of *ups*, *ced*, *tfb3* and *cdc6–2* genes. (**A**) EMSA analysis of Csa3a binding to the *upsX* (SiRe_1878), *upsE* (SiRe_1879), *upsA* (SiRe_1881), *cedA1* (SiRe 1316), *cedB* (SiRe_1857), *tfb3* (SiRe_1717) and *cdc6–2* (SiRe_1231) promoters. For binding assays using the wild-type promoters or the mutated promoters, each reaction contained the 5′-end HEX labeled probes: 5 ng/µlL, poly(dI-dC): 5 ng/µl, and Csa3a protein: 40, 80 or 120 ng/µl. For the specific competition assay, each reaction contained the 5′-end HEX labeled probes: 5 ng/µl, poly(dI-dC): 5 ng/µL, and Csa3a protein: 120 ng/µL, and unlabeled specific competitor (cold probe): 10 or 20 ng/µL. The probe location and mutated region on each promoter are indicated in relation to the ATG codon of each open reading frame. The wild-type and mutated sequences are indicated and the UV-responsive element (26) is boxed. P and PM: the wild-type probes and the mutated probes used in EMSA and LSPR experiments, respectively. W: precipitation at loading wells; S: shift; F: free probe. (**B**) LSPR analysis of fixed Csa3a protein on the chip to bind the promoters and their mutants used in (**A**). The concentrations of probes used for the analysis are shown. K_D = mean±standard derivations of three independent experiments.
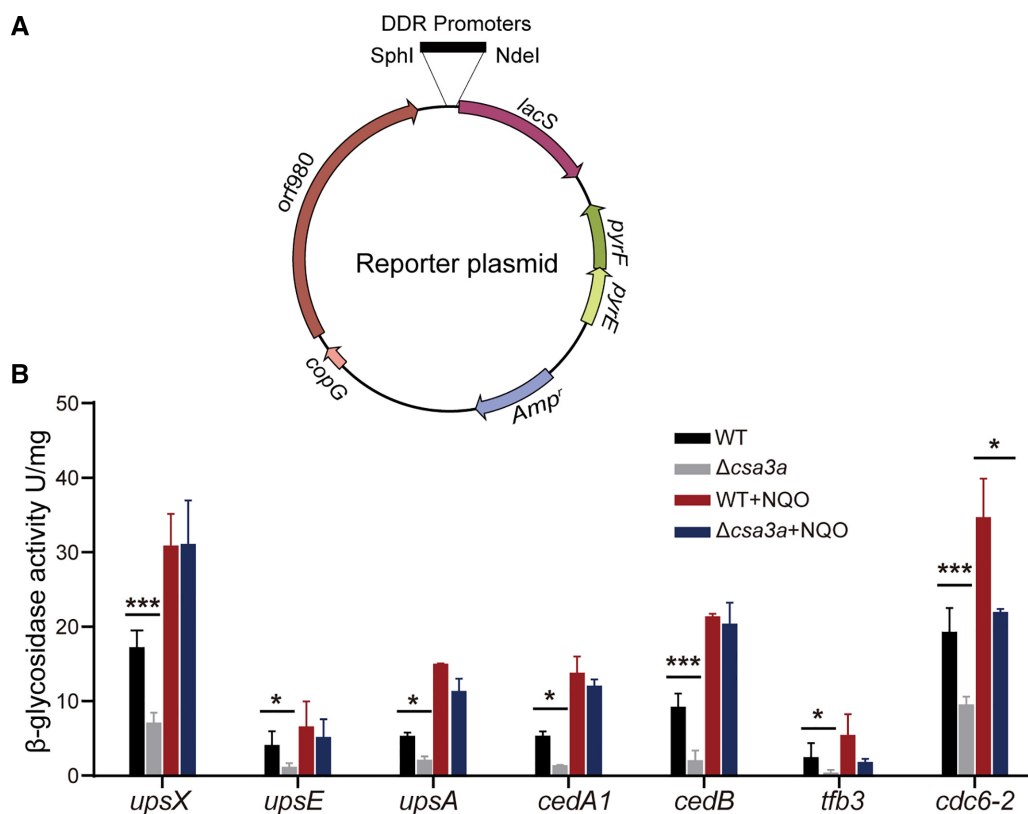
Figure 3. Analysis of promoter activities using the reporter gene system in the strains with or without *csa3a* gene. (**A**) The reporter plasmid used in this study. Promoters of DDR genes were cloned immediately upstream of *lacS* gene which encodes β-galactosidase. (**B**) The specific β-galactosidase activities for the tested promoters in wild-type (*S. islandicus* E233S) or *csa3a* deletion strains with or without treatment with 2 μM NQO for 6 h. Error bars: standard derivations of three independent experiments. Statistical significance: *$P < 0.05$, ***$P < 0.001$, two-way ANOVA and Dunnett.

with two chromosomes post NQO treatment (Figure 5A), indicating these strains exhibited stronger DNA repair activity. However, nearly all *cdc6-2* deletion cells transformed into the DNA-less cells, showing cell death under the NQO treatment (Figure 5A). Importantly, more DNA fragments were observed in *csa3a* deletion strain from 6 to 48 hours post NQO treatment compared with the wildtype (Figure 5A), indicating a lower DNA repair efficiency in the *csa3a* deletion mutant.

The growth curves of the strains treated the same in Figure 5A showed that the culture containing 2 μM NQO could completely inhibit the growth of the Δ*csa3a* and Δ*cdc6-2* strains, whereas, for the wild-type strain, no obvious growth defect was observed (Figure 5B, Supplementary Table S8). From these findings, the deletions of *csa3a* and *cdc6-2* genes showed hypersensitivity to the NQO treatment. The plate titration experiment also confirmed that the amount of viable cells in the Δ*csa3a* culture treated with NQO for 24 h with 10-fold dilutions was lower than that of wild-type strain with the same treatment and at the same dilutions (Figure 5C). We also evaluated the sensitivity of the wild-type and Δ*csa3a* strains to NQO by determining their survival rate on plates after 2 μM NQO treatment for 6 h. The number of viable cells, estimated by their colony formation units (CFU), revealed that NQO-treated cultures exhibited a strong reverse correlation to the drug concentration for both wild-type and Δ*csa3a* strains (raw data shown

in Supplementary Table S9). However, the viable rate of the Δ*csa3a* strain was significantly lower than that of the wild-type strain (Figure 5D). In summary, the *csa3a* gene deletion significantly elevated the sensitivity of *S. islandicus* cells to the DNA damage reagent.

Csa3a is important for regulation of Ups- and Ced-mediated repair of CRISPR-damaged host genomic DNA

To study whether the Csa3a factor is involved in the regulation of Ups- and Ced-mediated repair of CRISPR-damaged host genomic DNA, we designed a targeting plasmid (pT*cas5*) against *cas5* gene in the wt (Δ*pyrEF*Δ*lacS*) or Δ*csa3a* (Δ*pyrEF*Δ*lacS*Δ*csa3a*) cells, then, used a *cas5* deletion strain (Δ*pyrEF*Δ*lacS*Δ*cas5*) as the mating partner cells to provide repair donor DNA. Plasmid pT*cas5* was electroporated into wt or Δ*csa3a* cells (resulting in wt::pT*cas5* or Δ*csa3a*::pT*cas5*), after which these cells were incubated either in presence or absence of Δ*cas5* cells (Figure 6A). The genomic DNA of transformants carrying pT*cas5* plasmids was targeted at the *cas5* gene locus (Figure 6B). However, if Ups and Ced systems import genomic DNA of Δ*cas5* mating partner cells into the wt or Δ*csa3a* cells carrying pT*cas5* plasmid (the conjugants of wt::pT*cas5* × Δ*cas5* or Δ*csa3a*::pT*cas5* × Δ*cas5*), the damaged DNA was repaired through homologous recombination pathway (Figure 6B). Moreover, since the donor DNA carried a deletion at the
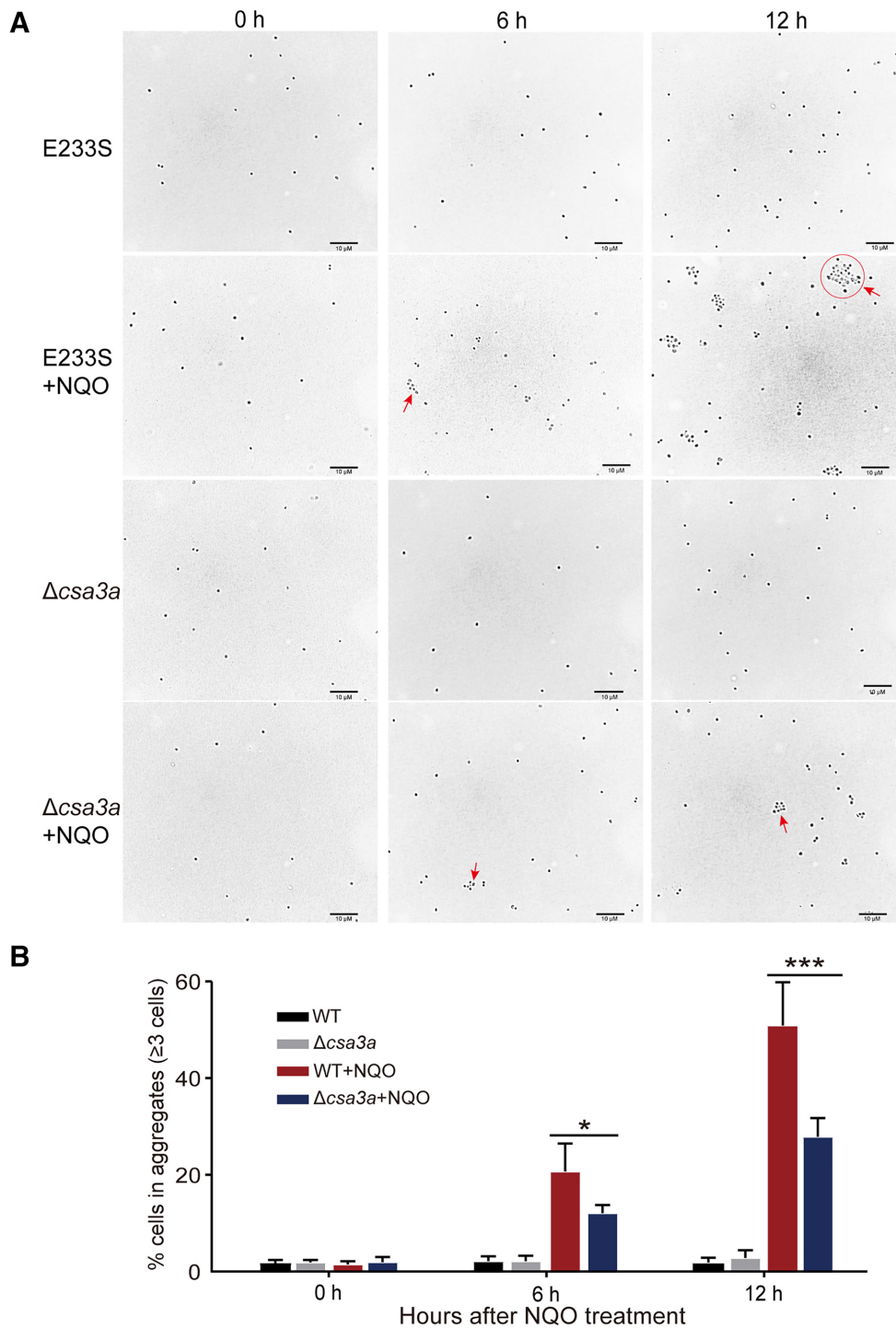
Figure 4. Deletion of *csa3a* gene reduced DNA damage-induced cell aggregation. (**A**) Microscopic analysis of cell aggregates in samples taken from the cultures of the wild-type (E233S) and Δ*csa3a* mutants at different time points with or without NQO treatment. Red arrows indicate the example of cell aggregates, and the aggregate with more than 30 cells in the E233S sample at 12 h post NQO treatment was circled. (**B**) Quantification data of cell aggregates in the cell samples shown in panel A. At least 1000 cells were analyzed for each sample. Error bars: standard derivations of three independent experiments. Statistical significance: *$P < 0.05$, ***$P < 0.001$, two-way ANOVA and Dunnett.

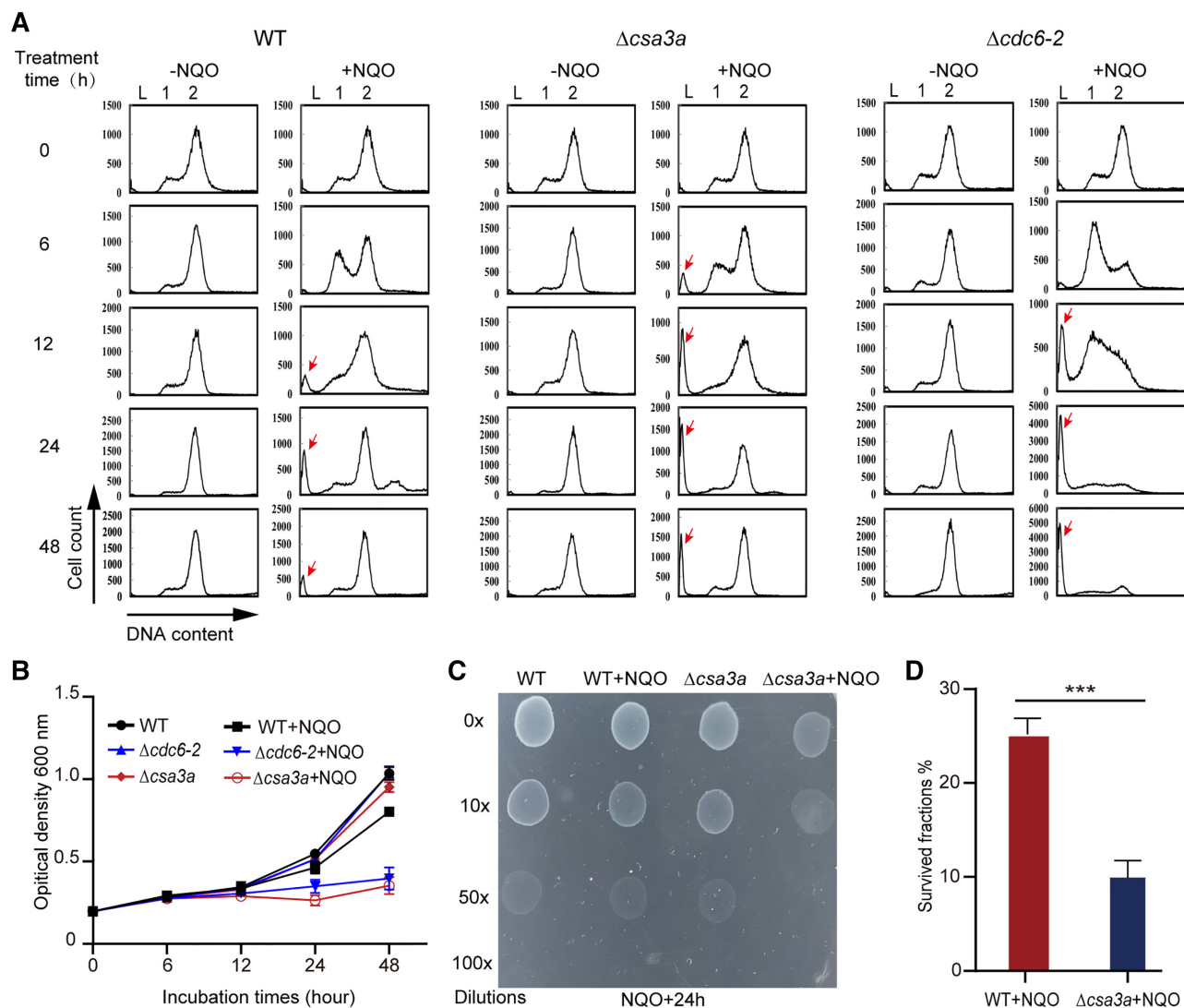**Figure 5.** The *csa3a* deleted strain showed higher sensitivity to NQO. (**A**) Cell cycle profiles of wild-type, Δ*csa3a* and Δ*cdc6-2* cultures. DNA contents were divided into 256 arbitrary points on the X-axis, and cell counts (Y-axis) were obtained for each point and plotted against the DNA content. Each sample was grown in SCVU in the presence (denoted as +NQO), or absence (–NQO) of 2 μM NQO for 6 h. DNA-less cells (L); cells containing one chromosome (1), and cells containing two chromosomes (2). Red arrows indicate the DNA-less cells. (**B**) Growth curves based on absorbance at 600 nm. (**C**) Plate titration of cells. Each strain was grown in the absence or presence of NQO for 48 h, and a series of dilutions were prepared for each sample which was plated for 12 h. WT: *S. islandicus* E233S; Δ*cas3a*: *csa3a* deletion strain; Δ*cdc6-2*: *cdc6-2* deletion strain. Error bars: standard derivations of three independent experiments. (**D**) Survival rates of *S. islandicus* wild-type (E233S) and Δ*csa3a* strains after NQO treatment. Exponentially growing strains were treated with 2 μM NQO for 6 h. Cell samples were plated on NQO-free SCVYU plates for determination of colony formation units (CFU)/mL culture. Survival rate = (CFU/mL of NQO treated cells)/(CFU/ml of non-treated cells). Statistical significance: ***P < 0.001, two-way ANOVA and Dunnett.

cas5 gene locus, the repaired DNA would not be further targeted (Figure 6B). Transformation of the self-targeting plasmid pT*cas5* resulted in 10^2- to 10^3-folds lower transformation efficiency compared with the transformation of the control plasmid pSeSD (Supplementary Table S10). Transformation efficiency of wt::pT*cas5* and Δ*csa3a*::pT*cas* were $3.05–4.40 × 10^2$ and $3.30 × 10^2$ cfu/μg plasmid DNA, respectively (Supplementary Table S10). While, transformation efficiency of wt::pT*cas5* × Δ*cas5* and Δ*csa3a*::pT*cas5* × Δ*cas5* were $5.42–8.35 × 10^3$ and $3.42–3.60 × 10^3$ cfu/μg plasmid DNA, respectively (Supplementary Table S10). Therefore, for both wt and Δ*csa3a* cells transformed with pT*cas5*, their transformation efficiencies increased by more

than 10-folds when incubated with Δ*cas5* mating partner cells (Figure 6C). Together with previous reports that deletion of *ups* and *ced* genes failed to transfer DNA for DNA damage repair in *Sulfolobus* cells treated with UV light (16,27), our result indicated that the Ups and Ced systems mediated DNA damage repair at the targeted *cas5* gene locus. Notably, *csa3a* gene deletion showed significantly lower repair efficiency (Figure 6C), an indication that the *csa3a* gene is critical for regulation of Ups- and Ced-mediated repair of CRISPR-damaged host genomic DNA.

To reveal on DNA exchange and homologous recombination, PCR was performed on the colonies of conjugants obtained in mixtures of wt::pT*cas5* × Δ*cas5* or
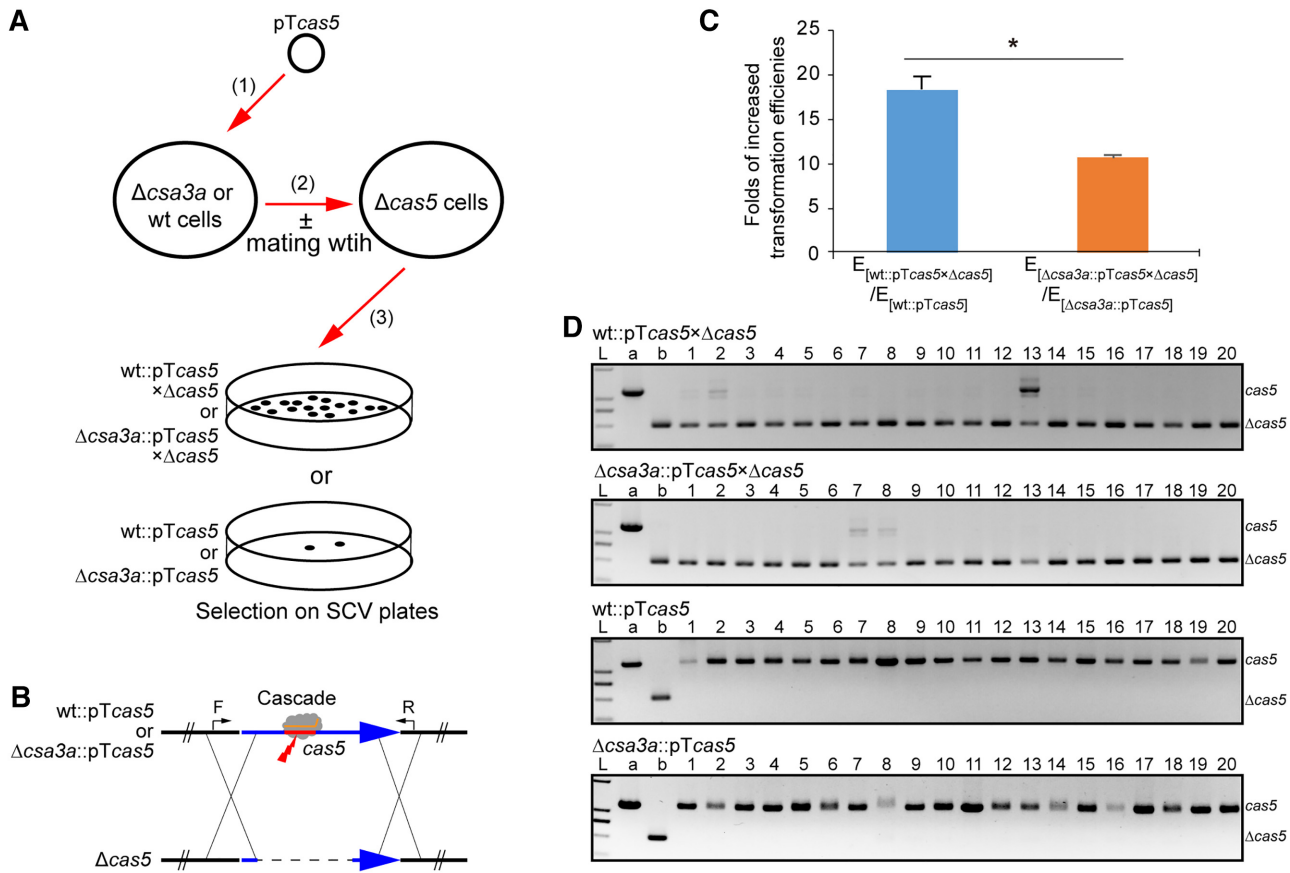
Figure 6. Deletion of *csa3a* gene reduced the efficiency of Ups- and Ced-mediated repair of CRISPR-damaged host genomic DNA. (**A**) schematic diagram of Ups- and Ced-mediated DNA repair analysis. Plasmid pT*cas5* carrying a mini-CRISPR (Repeat-Spacer-Repeat) with the spacer against *cas5* gene was electroporated into *S. islandicus* wt (Δ*pyrEF*Δ*lacS*) and Δ*csa3a* (Δ*pyrEF*Δ*lacS*Δ*csa3a*) cells (step 1). After electroporation, the transformed cells were incubated with or without Δ*cas5* (Δ*pyrEF*Δ*lacS*Δ*cas5*) mating partner cells for 2 h at 78°C (step 2) and then plated in the plates of SCV medium without uracil (step 3). (**B**) schematic diagram of homologous recombination of CRISPR-damaged genomic DNA in wt or Δ*csa3a* cells carrying the pT*cas5* self-targeting plasmid and containing the donor DNA imported from Δ*cas5* cells. Subtype I-A Cascade complex targeted site at *cas5* gene locus is shown in red. The *cas5* gene indicates as a blue arrow. Deletion of the *cas5* gene is indicated as a dash line. Double-crossover between the homologous regions upstream and downstream of *cas5* gene is shown. F and R represent the primers used for PCR amplification of the *cas5* gene locus on the chromosome of the colonies. (**C**) fold increases of the transformation efficiencies of wt or Δ*csa3a* cells incubated with Δ*cas5* mating partner cells compared with that of wt or Δ*csa3a* cells ($E_{[\mathrm{wt::pT}cas5 \times \Delta cas5]}/E_{[\mathrm{wt::pT}cas5]}$ or $E_{[\Delta csa3a::\mathrm{pT}cas5 \times \Delta cas5]}/E_{[\Delta csa3a::\mathrm{pT}cas5]}$; E: transformation efficiency) were calculated, respectively. Statistical significance: *$P < 0.05$, two-way ANOVA and Dunnett. (**D**) PCR amplification of the *cas5* gene locus on the chromosomes of 20 randomly selected wt::pT*cas5* × Δ*cas5*, Δ*csa3a*::pT*cas5* × Δ*cas5*, wt::pT*cas5* and Δ*csa3a*::pT*cas5* single colonies, respectively, on SCV plates without addition of uracil. L, DNA ladder; a, PCR control using *S. islandicus* REY15A genomic DNA as the template; b, PCR control using the Δ*cas5* strain genomic DNA as the template; 1–20, PCR amplification of *cas5* gene locus using 20 randomly selected colonies, respectively.

Δ*csa3a*::pT*cas5* × Δ*cas5* strains. We studied the genotype of 20 randomly selected colonies per mixture. PCR analysing the plasmid region containing the mini-CRISPR cassette revealed that all these colonies carried the pT*cas5* plasmid (Supplementary Figure S2), and also indicated no Δ*cas5* colonies formed on SCV plates without addition of uracil. We obtained 20/20 and 20/20 of randomly selected single colonies carrying the *cas5* gene deletion in wt::pT*cas5* × Δ*cas5* and Δ*csa3a*::pT*cas5* × Δ*cas5*, respectively (Figure 6D). Sequencing result revealed that these deletions on the genomic DNA exactly matched with the deletion region on the Δ*cas5* mating partner cells. PCR analysing the colonies of wt::pT*cas5* and Δ*csa3a*::pT*cas5* transformants showed intact *cas5* gene on their chromosomes, indicating that these colonies escaped CRISPR immunity (Figure 6D). However, mutations were not identified at the mini-CRISPR cassette on the plasmid of these colonies, suggest-

ing mutations occurred at the *cas* gene loci on the chromosome. Based on these findings, it is evident that Csa3a regulates Ups and Ced systems to repair CRISPR-damaged host genomic DNA in *S. islandicus*.

DISCUSSION

Environmental factors, such as UV and other types of radiation, can cause DNA damage in the form of strand breaks, which are particularly lethal and can be mutagenic. The hyperthermophilic archaeon Sulfolobales genus encodes the Ups and Ced, the special DNA damage repair system (16). The *ups* operon encodes 5 proteins integrating to build the type IV pili (Figure 1B). The *ced* operon (*cedA1*, *cedA*, *cedA2* and *cedB*) encodes transmembrane proteins (Figure 1C). For instance, the *cedA1* and *cedA2* encode two small transmembrane proteins, *cedA* encodes a larger transmem-
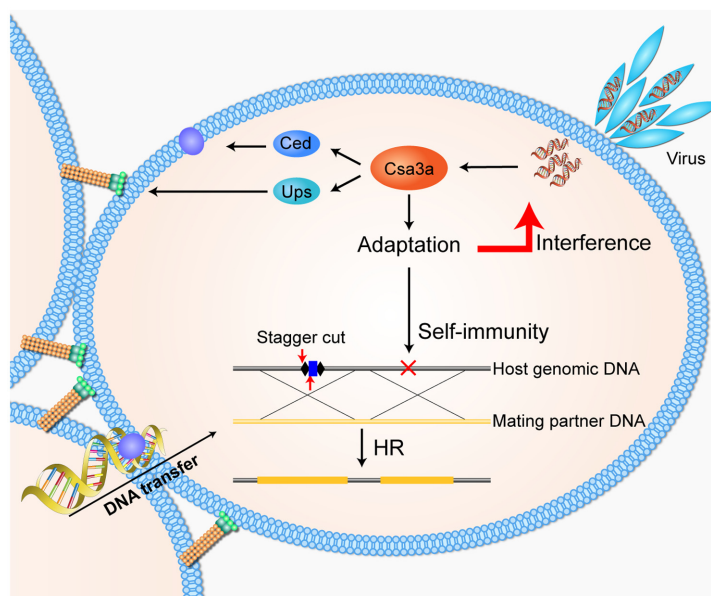
Figure 7. A proposal for Csa3a-centered network of DNA damage response for CRISPR immunity in *S. islandicus*. MGE invasion activates the expression of the global regulator Csa3a (32). Csa3a in turn activates expression of DDR genes, including *ups* and *ced* operons, and triggers CRISPR adaptation and immunity against invaders (7,8). However, a subset of host DNA derived spacers would guide self-immunity against the genomic DNA. The activated Ups system aggregates cells and the Ced system transfers DNA from adhered cells into the target cells. The transferred DNA was used as the donor DNA for homologous recombination (HR) to remove newly integrated spacers and to repair the DNA breaks, resulting in intact genomic DNA. Ups: UV-responsive pili of *Sulfolobus*; Ced: Crenarchaeal system for exchange of DNA. Diamond: the CRISPR repeat sequence.

brane protein, whereas *cedB* encodes a HerA/VirB4 homolog (16). UV-induced DNA damage up-regulates these *ups* genes, resulting in pili formation thereby causing cells to aggregate (17,18,27–30). Notably, the aggregations are species-specific mating pairs (17). VirB4/HerA homolog of the Ced system is, in most cases, highly up-regulated in *S. islandicus* after DNA damage (19,21), and is induced by overexpression of the CRISPR-associated factor Csa3a (8) (Supplementary Table S4). Furthermore, VirB4-ATPases are associated with conjugative type-IV secretion systems in bacteria, where they are essential for DNA transfer (16). Homologs of these genes are specific for the Crenarchaeota and can be found in most species of Sulfolobales, Acidilobales, and Desulfurococcales (16). Otherwise, this system functions as a DNA importer and plays an important role in DNA homologous recombination repair (16). CedA proteins are thought to assemble a membrane pore through which the DNA can be transferred (16). Membrane-bound ATPase CedB presumably binds the DNA and energizes the translocation (16). Once the DNA is introduced, it can potentially repair the extensive DNA damage caused by UV through homologous recombination (16,17,31).

Ups-Ced-mediated DNA damage repair is regulated during exposure to UV radiation. Since DNA transfer requires both Ups and Ced proteins, it makes more sense to use a common factor to regulate the two systems. In a previous study, *S. islandicus* Cdc6–2 protein was confirmed to specifically bind to the promoters of the *ups* and *ced* genes, thereby facilitating the expression of these genes (21). However, a higher Cdc6–2 expression level is essential but not sufficient to trigger DDR regulation in this archaeon (21). TFB3, a truncated version of the archaeal transcription fac-

tor B family proteins, has been found to regulate both Ups and Ced systems (19,20), downstream of Cdc6–2 regulation in the DDR network in *S. islandicus* (21).

In our previous work, we identified Csa3a as a transcriptional regulator that activates the expression of adaptation *cas* genes (7) and enhances transcription of CRISPR RNAs (8). Besides, the expression of the Csa3a activator is induced by an unknown mechanism upon invasion by mobile genetic elements (32). Therefore, Csa3a was thought to be a dedicated factor specific to CRISPR−Cas regulation (33). However, Csa3a-triggered CRISPR adaptation integrates a few (7.0%) host spacers into CRISPR arrays (8), inducing self-immunity. In addition, the adaptation of host self-DNA occurred in other model systems. For example, in *de novo* spacer acquisition process, 32%, 16% and 22.8% or 1.8% (for induction or non-induction of Cas1, Cas2 expression, respectively) of new spacers have been derived from host genomic DNA in *S. thermophilus* subtype II-A (10), *Pectobacterium atrosepticum* subtype I-F (34) and *E. coli* subtype I-E (9) systems. Even in primed acquisition processes, 0.01– 0.03% of new spacers have been derived from host genomic DNA in *E. coli* subtype I-E (35) and *P. atrosepticum* subtype I-F (34) systems. This raises an important question on how the cells evade self-immunity guided by self-derived spacers. Of note, CRISPR−Cas systems have developed diverse mechanisms to evade autoimmunity. For instance, bacterial and archaeal genomes encode anti-CRISPR proteins to inhibit CRISPR immunity (36–39), therefore, reduce the threats to host genomic DNA.

In this study, our results revealed that the CRISPR-associated factor Csa3a of *S. islandicus* could specifically bind to the promoters of DDR genes, including *ups*, *ced*,

tfb3 and *cdc6–2 in vitro* (Figure 2), and deletion of the *csa3a* gene significantly suppressed the expression of these genes (Table 1 and Figure 3), reducing the formation of cell aggregates (Figure 4). As a result, deletion of *csa3a* gene increased the sensitivity of cells to the DNA-damaging reagent NQO (Figure 5). Analysis of the transcriptome data revealed that DDR genes were lower in *csa3a* deletion strain compared with the wild-type without NQO treatment (Table 1), indicating Csa3a activates DDR expression. Notably, all DDR genes were significant higher in Δ*csa3a* cells treated with NQO than in cells not treated with NQO (Table 1). This implies that the Cdc6-2 and TFB3-signaling pathway became dominant when cells were treated with a DNA-damaging reagent (19,21). Moreover, Csa3a regulated the expression of *cdc6-2* and *tfb3* genes (Table 1 and Figure 2), suggesting Cdc6-2 and TFB3 are involved in Csa3a-mediated regulation of DDR genes.

Our further experiments confirmed that CRISPR-damaged host genomic DNA was repaired through mating with the *Sulfolobus* cells lacking the CRISPR targeting region (Figure 6), inferring the involvement of the Ups and Ced systems in this process. Importantly, deletion of *csa3a* gene resulted in reduced repair efficiency (Figure 6), indicating the Csa3a factor played an important regulatory role in the DNA damage repair process. Moreover, loss of newly adapted spacer during virus infection was detected in *S. islandicus* (40), implying the single strand nicks generated at leader-repeat region during spacer acquisition could also induce homologous recombination probably through the Ups-Ced pathway. Therefore, we propose a model for this regulation (Figure 7): (i) MGE invasion activates Csa3a expression (32), (ii) Csa3a triggers CRISPR adaptation and CRISPR RNA transcription (7,8), (iii) self-spacers guide immunity against host DNA, (iv) Csa3a activates the expression of Ups, Ced and DNA repair genes, (v) Ups system mediated cell aggregations and Ced system transfer genomic DNA into damaged cells (16–18,28,30), (vi) homologous recombination repair occurred at the DNA breaks of the target sites and leader-proximal regions, resulting in repair of targeted sites and loss of new spacers. This model well explains the interplay between the Csa3a functions in triggering CRISPR adaptation and activation of the DNA repair systems, and expands our understanding of the lost link between CRISPR self-immunity and genome stability.

DATA AVAILABILITY

Transcriptome data were deposited in the SRA database under Accession PRJNA608153.

SUPPLEMENTARY DATA

Supplementary Data are available at NAR Online.

ACKNOWLEDGEMENTS

FUNDING

Conflict of interest statement. None declared.

REFERENCES

1. Barrangou,R., Fremaux,C., Deveau,H., Richards,M., Boyaval,P., Moineau,S., Romero,D.A. and Horvath,P. (2007) CRISPR provides acquired resistance against viruses in prokaryotes. *Science*, **315**, 1709–1712.
2. Makarova,K.S., Haft,D.H., Barrangou,R., Brouns,S.J., Charpentier,E., Horvath,P., Moineau,S., Mojica,F.J., Wolf,Y.I., Yakunin,A.F. *et al.* (2011) Evolution and classification of the CRISPR–Cas systems. *Nat. Rev. Microbiol.*, **9**, 467–477.
3. Koonin,E.V., Makarova,K.S. and Zhang,F. (2017) Diversity, classification and evolution of CRISPR–Cas systems. *Curr. Opin. Microbiol.*, **37**, 67–78.
4. Charpentier,E., Richter,H., van der Oost,J. and White,M.F. (2015) Biogenesis pathways of RNA guides in archaeal and bacterial CRISPR–Cas adaptive immunity. *FEMS Microbiol. Rev.*, **39**, 428–441.
5. Plagens,A., Richter,H., Charpentier,E. and Randau,L. (2015) DNA and RNA interference mechanisms by CRISPR–Cas surveillance complexes. *FEMS Microbiol. Rev.*, **39**, 442–463.
6. Yosef,I., Goren,M.G. and Qimron,U. (2012) Proteins and DNA elements essential for the CRISPR adaptation process in *Escherichia coli. Nucleic. Acids. Res.*, **40**, 5569–5576.
7. Liu,T., Li,Y., Wang,X., Ye,Q., Li,H., Liang,Y., She,Q. and Peng,N. (2015) Transcriptional regulator-mediated activation of adaptation genes triggers CRISPR *de novo* spacer acquisition. *Nucleic Acids Res.*, **43**, 1044–1055.
8. Liu,T., Liu,Z., Ye,Q., Pan,S., Wang,X., Li,Y., Peng,W., Liang,Y., She,Q. and Peng,N. (2017) Coupling transcriptional activation of CRISPR–Cas system and DNA repair genes by Csa3a in *Sulfolobus islandicus. Nucleic Acids Res.*, **45**, 8978–8992.
9. Levy,A., Goren,M.G., Yosef,I., Auster,O., Manor,M., Amitai,G., Edgar,R., Qimron,U. and Sorek,R. (2015) CRISPR adaptation biases explain preference for acquisition of foreign DNA. *Nature*, **520**, 505–510.
10. Wei,Y., Terns,R.M. and Terns,M.P. (2015) Cas9 function and host genome sampling in Type II-A CRISPR–Cas adaptation. *Genes Dev.*, **29**, 356–361.
11. Shiimori,M., Garrett,S.C., Chambers,D.P., Glover,C.V.C. 3rd, Graveley,B.R. and Terns,M.P. (2017) Role of free DNA ends and protospacer adjacent motifs for CRISPR DNA uptake in *Pyrococcus furiosus. Nucleic Acids Res.*, **45**, 11281–11294.
12. Kreuzer,K.N. (2013) DNA damage responses in prokaryotes: regulating gene expression, modulating growth patterns, and manipulating replication forks. *Cold Spring Harb. Perspect. Biol.*, **5**, a012674.
13. Sirbu,B.M. and Cortez,D. (2013) DNA damage response: three levels of DNA repair regulation. *Cold Spring Harb. Perspect. Biol.*, **5**, a012724.
14. Baharoglu,Z. and Mazel,D. (2014) SOS, the formidable strategy of bacteria against aggressions. *FEMS Microbiol. Rev.*, **38**, 1126–1145.
15. Erill,I., Campoy,S. and Barbe,J. (2007) Aeons of distress: an evolutionary perspective on the bacterial SOS response. *FEMS Microbiol. Rev.*, **31**, 637–656.
16. van Wolferen,M., Wagner,A., van der Does,C. and Albers,S.V. (2016) The archaeal Ced system imports DNA. *Proc. Natl. Acad. Sci. U.S.A.*, **113**, 2496–2501.
17. Ajon,M., Frols,S., van Wolferen,M., Stoecker,K., Teichmann,D., Driessen,A.J., Grogan,D.W., Albers,S.V. and Schleper,C. (2011) UV-inducible DNA exchange in hyperthermophilic archaea mediated by type IV pili. *Mol. Microbiol.*, **82**, 807–817.
18. Frols,S., Ajon,M., Wagner,M., Teichmann,D., Zolghadr,B., Folea,M., Boekema,E.J., Driessen,A.J., Schleper,C. and Albers,S.V. (2008) UV-inducible cellular aggregation of the hyperthermophilic

archaeon *Sulfolobus solfataricus* is mediated by pili formation. *Mol. Microbiol.*, **70**, 938–952.

19. Feng,X., Sun,M., Han,W., Liang,Y.X. and She,Q. (2018) A transcriptional factor B paralog functions as an activator to DNA damage-responsive expression in archaea. *Nucleic Acids Res.*, **46**, 7085–7096.

20. Schult,F., Le,T.N., Albersmeier,A., Rauch,B., Blumenkamp,P., van der Does,C., Goesmann,A., Kalinowski,J., Albers,S.V. and Siebers,B. (2018) Effect of UV irradiation on *Sulfolobus acidocaldarius* and involvement of the general transcription factor TFB3 in the early UV response. *Nucleic Acids Res.*, **46**, 7179–7192.

21. Sun,M., Feng,X., Liu,Z., Han,W., Liang,Y.X. and She,Q. (2018) An Orc1/Cdc6 ortholog functions as a key regulator in the DNA damage response in Archaea. *Nucleic Acids Res.*, **46**, 6697–6711.

22. Deng,L., Zhu,H., Chen,Z., Liang,Y.X. and She,Q. (2009) Unmarked gene deletion and host-vector system for the hyperthermophilic crenarchaeon *Sulfolobus islandicus*. *Extremophiles*, **13**, 735–746.

23. Han,W., Xu,Y., Feng,X., Liang,Y.X., Huang,L., Shen,Y. and She,Q. (2017) NQO-induced DNA-less cell formation is associated with chromatin protein degradation and dependent on A0A1-ATPase in *Sulfolobus*. *Front. Microbiol.*, **8**, 1480.

24. Peng,N., Xia,Q., Chen,Z., Liang,Y.X. and She,Q. (2009) An upstream activation element exerting differential transcriptional activation on an archaeal promoter. *Mol. Microbiol.*, **74**, 928–939.

25. Peng,N., Deng,L., Mei,Y., Jiang,D., Hu,Y., Awayez,M., Liang,Y. and She,Q. (2012) A synthetic arabinose-inducible promoter confers high levels of recombinant protein expression in hyperthermophilic archaeon *Sulfolobus islandicus*. *Appl. Environ. Microbiol.*, **78**, 5630–5637.

26. Le,T.N., Wagner,A. and Albers,S.V. (2017) A conserved hexanucleotide motif is important in UV-inducible promoters in *Sulfolobus acidocaldarius*. *Microbiology*, **163**, 778–788.

27. van Wolferen,M., Ajon,M., Driessen,A.J. and Albers,S.V. (2013) Molecular analysis of the UV-inducible pili operon from Sulfolobus acidocaldarius. *Microbiologyopen*, **2**, 928–937.

28. Frols,S., Gordon,P.M., Panlilio,M.A., Duggin,I.G., Bell,S.D., Sensen,C.W. and Schleper,C. (2007) Response of the hyperthermophilic archaeon *Sulfolobus solfataricus* to UV damage. *J. Bacteriol.*, **189**, 8708–8718.

29. Gotz,D., Paytubi,S., Munro,S., Lundgren,M., Bernander,R. and White,M.F. (2007) Responses of hyperthermophilic crenarchaea to UV irradiation. *Genome Biol.*, **8**, R220.

30. Frols,S., White,M.F. and Schleper,C. (2009) Reactions to UV damage in the model archaeon *Sulfolobus solfataricus*. *Biochem. Soc. Trans.*, **37**, 36–41.

31. Rolfsmeier,M.L., Laughery,M.F. and Haseltine,C.A. (2010) Repair of DNA double-strand breaks following UV damage in three *Sulfolobus solfataricus* strains. *J. Bacteriol.*, **192**, 4954–4962.

32. Leon-Sobrino,C., Kot,W.P. and Garrett,R.A. (2016) Transcriptome changes in STSV2-infected *Sulfolobus islandicus* REY15A undergoing continuous CRISPR spacer acquisition. *Mol. Microbiol.*, **99**, 719–728.

33. Patterson,A.G., Yevstigneyeva,M.S. and Fineran,P.C. (2017) Regulation of CRISPR−Cas adaptive immune systems. *Curr. Opin. Microbiol.*, **37**, 1–7.

34. Staals,R.H., Jackson,S.A., Biswas,A., Brouns,S.J., Brown,C.M. and Fineran,P.C. (2016) Interference-driven spacer acquisition is dominant over naive and primed adaptation in a native CRISPR−Cas system. *Nat. Commun.*, **7**, 12853.

35. Savitskaya,E., Semenova,E., Dedkov,V., Metlitskaya,A. and Severinov,K. (2013) High-throughput analysis of type I-E CRISPR/Cas spacer acquisition in *E. coli*. *RNA Biol.*, **10**, 716–725.

36. Borges,A.L., Davidson,A.R. and Bondy-Denomy,J. (2017) The discovery, mechanisms, and evolutionary impact of anti-CRISPRs. *Annu. Rev. Virol.*, **4**, 37–59.

37. Bhoobalan-Chitty,Y., Johansen,T.B., Di Cianni,N. and Peng,X. (2019) Inhibition of type III CRISPR−Cas immunity by an archaeal virus-encoded anti-CRISPR protein. *Cell*, **179**, 448–458.

38. He,F., Bhoobalan-Chitty,Y., Van,L.B., Kjeldsen,A.L., Dedola,M., Makarova,K.S., Koonin,E.V., Brodersen,D.E. and Peng,X. (2018) Anti-CRISPR proteins encoded by archaeal lytic viruses inhibit subtype I-D immunity. *Nat. Microbiol.*, **3**, 461–469.

39. Athukoralage,J.S., McMahon,S.A., Zhang,C., Gruschow,S., Graham,S., Krupovic,M., Whitaker,R.J., Gloster,T.M. and White,M.F. (2020) An anti-CRISPR viral ring nuclease subverts type III CRISPR immunity. *Nature*, **577**, 572–575.

40. Erdmann,S., Le Moine Bauer,S. and Garrett,R.A. (2014) Inter-viral conflicts that exploit host CRISPR immune systems of *Sulfolobus*. *Mol. Microbiol.*, **91**, 900–917.